Available online at www.sciencedirect.com
SCIENCE DIRECT®
Polymer 45 (2004) 171–179
polymer
www.elsevier.com/locate/polymer

Structural details, viscoelastic and mechanical response in blends of a vinyl alcohol-ethylene copolymer and a metallocenic ethylene-1-octene copolymer

M.L. Cerrada*, M.F. Laguna, R. Benavente, E. Pérez

Instituto de Ciencia y Tecnología de Polímeros (CSIC), Calle Juan de la Cierva 3, 28006 Madrid, Spain

Received 19 May 2003; received in revised form 6 October 2003; accepted 29 October 2003

Abstract

Some structural details and the viscoelastic and mechanical response of blends of a vinyl alcohol-ethylene (VAE), and a metallocenic ethylene-1-octene copolymer (CEO), have been analyzed. Both copolymers exhibit crystalline lattices whose diffraction peaks and long spacings appear at very similar spacing intervals. More information about the crystalline region is obtained from differential scanning calorimetry (DSC) measurements due to the difference in melting temperatures found for each of them. In addition, DSC results point out an inhibition of the VAE crystallization with CEO presence that is cooling-rate dependent. A decrease of rigidity and yield stress is observed as CEO content increases in the blends. However, the changes found in the mechanical parameters are not as significant as the variation in oxygen permeability. This feature seems to be due to the disruption of intra and intermolecular hydrogen interactions.

Keywords: Vinyl alcohol-ethylene copolymer; Crystallization; Relaxation process

1. Introduction

Vinyl alcohol-ethylene (VAE) copolymers are semi-crystalline irrespectively of composition because of the capability of the two comonomers to be incorporated in the same crystal cell [1,2] though the crystalline lattice developed depends on both composition and thermal history [3,4]. VAE copolymers are also characterized by outstanding barrier properties to gases [5] like O_2, N_2 and CO_2 and to hydrocarbons. The content in the former comonomer is typically selected based upon requirements in gas barrier and aroma preserving properties and processability. Low ethylene content grades (i.e. 29 mol%) offer better barrier properties than high ethylene content grades (i.e. 44 mol%). Conversely, high ethylene content grades generally offer better processability. This rather low gas and hydrocarbons permeability leads to a steadily increasing demand for these copolymers in food, drug and cosmetic packaging applications and in new markets as plastic vehicle fuel tank or the nascent plastic beer bottle. However, VAE copolymers are highly sensitive to humidity which alters its resistance to oxygen permeation [5,6] and exhibit some processing deficiencies, like a poor thermoformability in consequence of their high crystallization kinetics [7]. Therefore, the combination of VAE copolymers with polyethylenes [5], polypropylenes [8,9], polyesters [10,11] and polyamides [12,13] has acquired a great interest from either an industrial or academic point of view to preserve the excellent barrier characteristics and solve performance lacks of these copolymers.

The use of metallocene catalysts has permitted the synthesis of the so-called plastomers [14]. This denomination is applied to ethylene-α-olefins copolymers where comonomer content is over around 5 mol% and with density lower than typical linear low density polyethylene, LLDPE. The 'plastomer' term refers to a polymeric material that exhibits the dual characteristic of plastic and elastomeric behavior. If comonomer content is high enough, about 8–10 mol%, crystallinity is significantly reduced and melting temperature goes down to around 60–70 °C. They exhibit moderate barrier properties [15,16] to oxygen and carbon dioxide though they are good barrier to water vapor,

* Corresponding author. Tel.: +34-91-5622900; fax: +34-91-5644853.
E-mail address: ictcg26@ictp.csic.es (M.L. Cerrada), mlcerrada@ictp.csic.es (M.L. Cerrada).

0032-3861/$ - see front matter © 2003 Elsevier Ltd. All rights reserved.
doi:10.1016/j.polymer.2003.10.095

resulting complementary to that transport behavior aforementioned for VAE copolymers.

This work seeks to comprehensively analyze the structure developed, relaxation processes and mechanical behavior exhibited by a commercial VAE copolymer and its blends with a metallocene ethylene-1-octene plastomer, CEO. Moreover, relationship of all of these characteristics will be established with those previously observed from the study of the thermal and oxygen transport properties [17]. Such an exhaustive analysis has required the use of different techniques: X-ray diffraction at either wide (WAXS) or small angle (SAXS); differential scanning calorimetry (DSC); scanning electronic microscopy (SEM); dynamic-mechanical thermal analysis (DMTA); uniaxial tensile stress–strain and microhardness measurements. A conclusion about the feasibility of using CEO as alternative for reducing VAE processing difficulties might be reached after performance of this extensive characterization depending upon properties exhibited by blends of different composition.

2. Experimental

2.1. Materials and film preparation

A commercially available VAE copolymer (from DuPont) containing a nominal 56 mol% in vinyl alcohol content was used with a commercial metallocenic catalyzed ethylene-1-octene copolymer (CEO) with a 9.3 mol% 1-octene content (supplied by Exxon Chemical) for obtaining blends with different compositions. Table 1 shows the characteristics of these ethylene copolymers, which have been studied in detail in previous works [4,18–20].

Blends with different content in CEO: 25, 50 and 75% in weight, labeled as VAE75CEO25, VAE50CEO50 and VAE25CEO75, respectively, were prepared in a Haake Rheocord 9000 at 210 °C and at 40 rpm for 10 min. After blending and homogenization of the two components, sheets specimens were obtained as films by compression molding in a Collin press between hot plates (210 °C) at a pressure of 2.5 MPa for 5 min and, subsequently, quenched at ambient temperature between steel plates cooled with water. The films were kept within olefinic bags and placed in a desiccator at room temperature just until the moment of performing a particular experiment to avoid their contact to environmental humidity. Neither temperature nor vacuum was applied to dessicator due to the effect of both variables on the structure and properties of VAE, as shown in our previous work [21].

2.2. Characterization of the samples

Wide- (WAXS) and small-angle X-ray (SAXS) diffraction patterns were recorded in the transmission mode in the beamline A2 at HASYLAB (Hamburg, Germany) employing synchrotron radiation (with $\lambda = 0.150$ nm). WAXS and SAXS profiles were acquired simultaneously during heating experiments, similar to those of the DSC, in time frames of 10 s. Two linear position-sensitive detectors were used. The WAXS one, at a distance of around 17 cm from the sample, was calibrated with the different diffractions of a crystalline PET sample, and it was found to cover the spacings range from 0.3 to 0.9 nm. The SAXS detector, at a distance of around 200 cm from the sample, was calibrated with the different orders of rat-tail cornea ($L = 65$ nm), and it was found to cover the spacings range from 5.5 to 50 nm. The diffraction profiles were normalized to the beam intensity and corrected for the detectors efficiency.

Scanning electron microscopy experiments were carried out in a XL30 ESEM PHILIPS equipment. Samples were cryofractured prior observations.

DSC experiments were recorded using a Perkin–Elmer DSC7 calorimeter connected to a cooling system and calibrated with different standards. The sample weights ranged from 6 to 9 mg and the heating rate used was 20 °C min^{-1}.

Viscoelastic properties were measured with a Polymer Laboratories MK II dynamic mechanical thermal analyzer working in the tensile mode. The real (E') and imaginary (E'') components of the complex modulus and the loss tangent (tan δ) of each sample were determined at 1, 3, 10 and 30 Hz, over a temperature range from − 150 to 150 °C, at a heating rate of 1.5 °C min^{-1}.

The uniaxial mechanical behavior was analyzed for VAE, CEO and the distinct blends. Dumb-bell shaped specimens with gauge dimensions 15 mm in length and 1.9 mm in width were punched out from the sheets with a standardized die. Thickness of specimens ranged from 0.3 to 0.4 mm. Tensile testing was carried out using an Instron Universal testing machine calibrated according to standard procedures. All of the specimens were drawn at a crosshead speed of 10 mm min^{-1} at room temperature. The different mechanical parameters were calculated from the stress–strain curve. At least four specimens were tested for each

Table 1
Characteristics of the commercial ethylene copolymers analyzed

Sample	Comonomer type	Comonomer content (mol%)	10^{-5} M_w	M_w/M_n	Density (g cm^{-3})	MFI (g 10 min^{-1})
VAE	Vinyl alcohol	56	–	–	1.150	16
CEO	1-octene	9.3	1.15	2.55	0.882	1.1

material and the mean values are reported. The errors in the mean values are less than 10%.

A Vickers indentor attached to a Leitz microhardness, MH, tester was used to carry out microindentation measurements. Experiments were undertaken at 20 °C. A contact load of 0.98 N and a contact time of 25 s were employed. MH values (in MPa) were calculated according to the relationship:

$$\mathrm{MH} = 2\sin 68^\circ P/d^2 \quad (1)$$

where P (in N) is the contact load and d (in mm) is the diagonal length of the projected indentation area.

3. Results and discussion

3.1. Crystalline structure

Fig. 1 shows the WAXS diffractograms of the different samples at room temperature. It can be observed that the profile of the pure VAE component corresponds to the pseudohexagonal crystalline modification of this copolymer [4]. On the other hand, the diagram for pure CEO reflects the rather small crystallinity (of the order of only 22%) due to its relatively high comonomer content [20]. It has to be taken into account that 1-octene comonomer is not able to enter into the crystalline lattice of polyethylene, thus leading to considerably reduced crystallinities as the comonomer content increases. On the contrary, vinyl alcohol and ethylene units are able to cocrystallize, so that VAE copolymers present always a relatively high crystallinity at any composition [4].

The X-ray diffractograms of the blends agree, within the experimental error, with those obtained from weighed addition of the two pure components. Therefore, each constituent crystallizes in its particular crystalline cell and a superposition of them is observed. The similarity of both lattices and, consequently, the overlap of the diffraction peaks arising from VAE and CEO at same spacing region does not allow separation into crystalline diffractions and the amorphous components in the blends and the further estimation of their X-ray crystallinity.

Long spacings are depicted in Fig. 2 for the two plain copolymers and their different blends. No much information can be deduced from its analysis stemming from the SAXS profiles. The corresponding values are rather close, with a small decrease from around 13.0 to 12.0 nm on passing from pure VAE to neat CEO. Therefore, these two types of crystallites developed in the blends overlap into the SAXS curves observed due to their similar long spacing values.

Additional knowledge about the crystalline structure of these blends can be attained from melting process of specimens by calorimetric measurements. The initial heating scan related to the first melting has been exclusively taken under consideration in the current work owed to our interest to associate the structure generated after film processing with its subsequent properties. Fig. 3 portrays the existence of two melting process in the blends confirming the preceding assumption of two individual crystalline lattices one for each component within the blend. The location of the melting temperature, T_m, concerning to CEO is kept rather constant at around 72 °C, whereas, that related to VAE component is depressed slightly in VAE75CEO25 and VAE50CEO50 and significantly in VAE25CEO75, as reported in Table 2. The shift of the T_m^{VAE} to lower temperature is dependent upon the crystallization conditions imposed to VAE25CEO75. Crystallization of polymers takes place at conditions far from the equilibrium, leading to the existence of a significant amorphous zone. For quenched samples, the fast cooling limits the development of crystallites. A slower cooling permits more amenable to crystallites perfection that increases as crystallization rate is decreased. In VAE25CEO75, the crystallization of the VAE

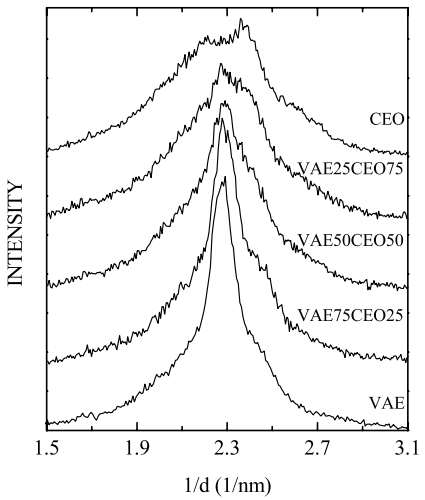

Fig. 1. X-ray diffraction patterns of the different samples at room temperature, shifted vertically for clarity.

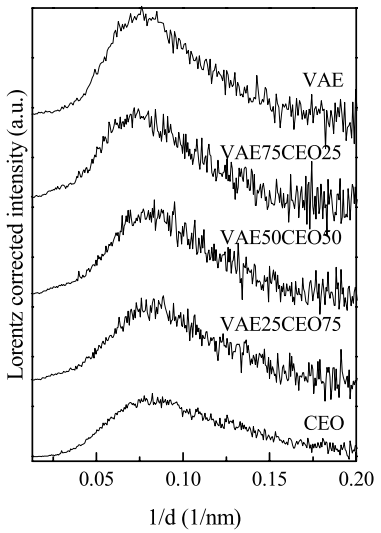

Fig. 2. Lorentz-corrected SAXS profiles for the different samples at ambient temperature, shifted vertically for clarity.

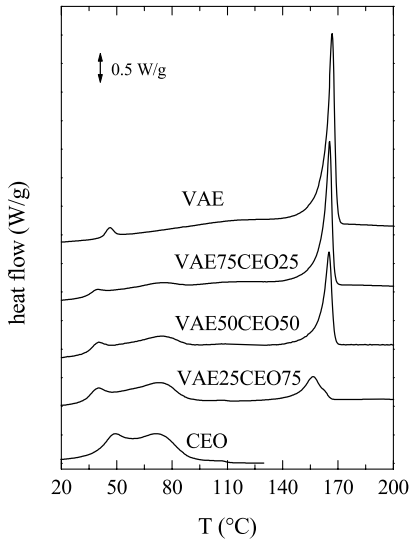

Fig. 3. DSC melting curves for the different samples (first heating run), shifted vertically for clarity.

component that occurred during molded processing is additionally hindered by CEO, which is the major constituent, and it seems that CEO partially inhibits it. Therefore, a diminishment is also observed in the value of its melting enthalpy normalized respect to the VAE content in the corresponding blend, ΔH_m^{VAE}, as found in other blends of CEO with iPP [22]. However, as crystallization is performed at 20 °C min^{-1} in the calorimeter, i.e. a cooling rate much slower to that applied by quenching along the film preparation, the subsequent melting of that structure better developed shows either that T_m^{VAE} is moved to higher temperatures or ΔH_m^{VAE} is slightly enlarged. Moreover, blend VAE25CEO75 displays a melting pattern in the VAE region, which is composed of two overlapped peaks indicating the development of two populations of crystallites with different perfection. Any additional knowledge about the crystal size cannot be achieved due to the closeness of long spacings for the two neat copolymers, as shown above.

No information can be attained from DSC experiment about the compatibility of the CEO and VAE amorphous phases in the blends. The glass transition temperature, T_g, is located for VAE copolymer at 55 °C while it is found at −47 °C in CEO [23] under the experimental conditions here used. The existence of a glass transition in this metallocenic CEO was also confirmed by modulated DSC measurements [23] and its location perfectly agrees with those temperatures found in similar copolymers [24]. In the blends, on the one hand, the T_g concerning the amorphous phase of CEO cannot be estimated due to its small intensity that rules out to distinguish it from noise of the equipment. On the other hand, the T_g related to the VAE amorphous regions completely overlaps with the melting process of CEO, as seen in Fig. 3. However, the immiscibility of these two components is clearly observed from the constancy of the location of the viscoelastic relaxation associated to the glass transition of each component, as will be discussed below.

Table 2
DSC values during first melting for the CEO and VAE components in the different samples

Sample	T_m^{CEO} (°C)	ΔH_{norm}^{CEO} (J/g)[a]	T_m^{VAE} (°C)	ΔH_{norm}^{VAE} (J/g)[a]
VAE	–	–	167	78 ± 1
VAE75CEO25	71	53 ± 1	165	72 ± 2
VAE50CEO50	72	52 ± 1	165	66 ± 2
VAE25CEO75	72	53 ± 1	157	62 ± 2
CEO	71	56 ± 1	–	–

[a] Normalized to either CEO or VAE content in the blend, respectively.

3.2. Viscoelastic behavior

Fig. 4 shows the viscoelastic response of the raw materials, VAE and CEO, and the blends. Four viscoelastic processes are exhibited in this VAE copolymer, at approximately, −125, −25, 60 and 118 °C (3 Hz) in loss tangent. These peaks are called as γ_{VAE}, β_{VAE}, α_{VAE} and α'_{VAE}, as referred previously [18,21]. On the other hand, in CEO only two well defined processes [20,25] are exhibited under tension (see Fig. 4) in the temperature range analyzed: γ_{CEO} and β_{CEO} in order of increasing temperatures. The relaxation traditionally observed at higher temperatures and labeled as α relaxation in polyethylene homopolymer and some ethylene-α-olefins copolymers with not very high comonomer content [26], is practically not detected in CEO in either tan δ or E'' curves. A small shoulder appearing at the high side of temperatures in the β_{CEO} process, seems be due to a strong overlapping of the α_{CEO} process with that

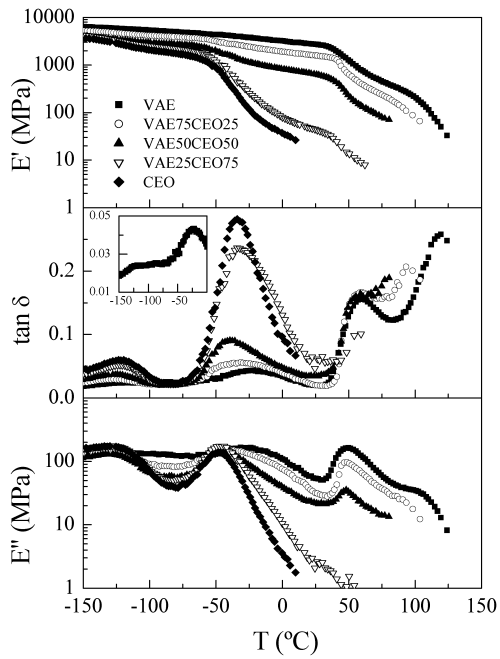

Fig. 4. Temperature dependence of the storage modulus (E'), loss modulus (E'') and loss tangent for the different specimens under study.

much more intense β_{CEO} relaxation. Since 1-octene content is high in CEO, there is a subsequent reduction in the amount and perfection of crystallites where the α relaxation takes place and, consequently, the process is shifted to very low temperature and a nearly complete merging with the β_{CEO} occurs [20]. It is expected, therefore, that its contribution will be almost insignificant in the blends. In spite of this just mentioned negligibility, a great complexity is observed in the viscoelastic response of these blends because of their multi-phasic nature and the motions that take place in each of these phases. On the one hand, the non-cocrystalization of the VAE and CEO in the same crystal lattice gives rise to two different crystalline phases and, on the other hand, the immiscibility of the distinct amorphous chains provokes the existence of two well-differentiated amorphous phases stemming from the corresponding ones in the semicrystalline copolymers, VAE and CEO.

Moreover, Fig. 4 also shows a clear dependence of the storage modulus, E', with the blend composition, being more significant from -50 °C to increasing temperatures, i.e. above the CEO glass transition [23,25]. The incorporation of the plastomer decreases significantly the rigidity. Consequently, E' also lowers as CEO content is raised since VAE copolymer is the stiffer component because of the establishment of intra and intermolecular hydrogen bonds within vinyl alcohol units. Therefore, those additional interactions become less important as VAE content diminishes in the blend, as reported in Table 3 for E' values at room temperature (23 °C). The analysis of the different relaxations observed is separately carried out as follows, in order of increasing temperatures.

The γ_{VAE} and γ_{CEO} relaxations corresponds to the observed γ relaxation in polyethylene, which was firstly attributed to crankshaft movements of polymethylenic chains [27]. There remains no clear consensus regarding the details of the underlying motional process [28,29]. There is, however, a body of opinions which support one or more of the various model for restricted conformational transitions as kink formation, inversion and migration [30–33]. Molecular dynamics simulations have been a powerful tool to corroborate the just mentioned nature of these conformational motions underlying the γ relaxation [34,35]. This type of motion requires chains containing sequences of three or more methylenic units, which are present in either VAE or CEO component. However, the relative low ethylene content in the VAE copolymer makes the intensity of this relaxation very weak in this constituent, as depicted in the insert of Fig. 4. Therefore, the intensity of this relaxation increases as CEO content in the blend does.

The β_{CEO} relaxation has been attributed to the glass transition [36–38] of polyethylene and its copolymers for some authors by molecular dynamics simulations. As aforementioned, experimental evidence has been reached by DSC and MDSC about the location of the glass transition at around -47 °C in the CEO and its glass fiber composites [23]. Accordingly, the β_{CEO} relaxation in CEO [25] and in its blends with VAE is considered as the relaxation process associated to the glassy–rubbery transition within the amorphous phase of this component.

The β_{VAE} relaxation is a very broad mechanism in the VAE copolymer analyzed. Therefore, this process overlaps considerably with that concerning the glass transition in CEO. This relaxation has been related to motions of chain units in the interfacial region [18,21] similarly to the relaxation universally detected at temperatures around -20 °C in branched ethylenes, in some samples of linear polyethylene and in various copolymers of ethylene with low comonomer contents [39,40].

The fact that these two β_{CEO} and β_{VAE} relaxations are overlapped makes convenient the separation of the loss curves into the different process contributing to the overall viscoelastic response to estimate more accurately their location. Fig. 5 depicts a well-description of tan δ magnitude of VAE75CEO25 quenched specimen as composed by distinct Gaussian curves, one for each observed relaxation process (also loss modulus curves can be fitted to this type of mathematical functions). Such a deconvolution does not have a theoretical basis that can explain satisfactorily the shape of the dependence of tan δ (or loss modulus) on temperature though some factors that can influence it are known. A method of curve deconvolution [41] has been proposed to analyze the dynamic mechanical loss curves in the region of the glass transition of several polymers, confirming the validity of this empirical approximation. In addition, it was shown that a Gaussian function provided the best fitting. As observed, the summation of five Gaussian curves for VAE75CEO25 blend provides a good overall fitting over the whole experimental temperature range measured. Therefore, this method constitutes a useful tool to determine the peak positions, which are listed in Table 3.

Table 3
Relaxation temperatures (tan δ basis, at 3 Hz) for the different processes, storage modulus values at room temperature and T_g estimation from E' for the neat copolymers and the different blends

Sample	$\gamma_{VAE} + \gamma_{CEO}$ (°C)	β_{CEO} (°C)	β_{VAE} (°C)	α_{VAE} (°C)	α'_{VAE} (°C)	$E'_{23\ °C}$ (MPa)	T_g^{CEO} (°C)	T_g^{VAE} (°C)
VAE	−128	–	−22	60	119	2750	–	45
VAE75CEO25	−128	−35	−22	59	96	1600	−51	44
VAE50CEO50	−126	−38	−18	59	–	650	−52	44
VAE25CEO75	−124	−33	−14	–	–	46	−50	40
CEO	−123	−34	–	–	–	–	−51	–

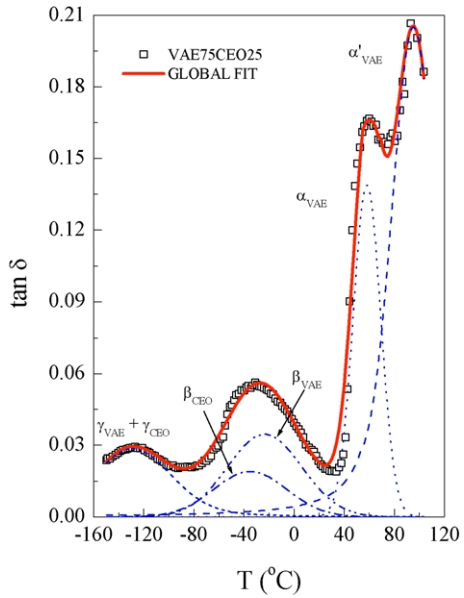

Fig. 5. Deconvolution of VAE70CEO25 loss tangent curve at 3 Hz (symbols) into five relaxation processes (dot lines) and the overall fit (solid line).

The α_{VAE} relaxation is considered as the glass transition of amorphous regions in the VAE copolymer. In the blends VAE75CEO25 and VAE50CEO50, the position of this relaxation remains practically unchanged indicating the immiscibility of the two constituents in these blends. This feature is also observed in the relaxation associated to the glass transition of the amorphous regions in CEO, though it is visually more ambiguous due to its merging with the β_{VAE} process. In VAE25CEO75, this relaxation is practically not detected in the loss curves, either E'' or tan δ. However, it is clearly observed in E'. It appears as a drop in the E' representation that is less intense than that related to the glass transition in CEO since this copolymer is the major component in that blend. In consequence, the mechanical resistance of VAE25CEO75 close to T_g of VAE is very low and the measurements under tension cannot be performed at those temperatures. The value estimated for T_g^{VAE} from E' is slightly decreased respect to those found in the other two blends and neat VAE. This feature joined to the fact of the diminishment in crystallinity mentioned along first melting seems to point out, in addition to the crystallite inhibition, that for this composition incompatibility of the amorphous regions of the two components is not as complete as for VAE75CEO25 and VAE50CEO50 blends.

The intensity of the α_{VAE} process is also kept unaffected for the neat VAE copolymer and the VAE75CEO25 and VAE50CEO50 blends. The crystallinity developed in these three polymeric systems is practically the same and, consequently, the motion restrictions existing in the amorphous regions stemming from the VAE component are in practice similar for these specimens mentioned.

The VAE copolymer under study and the blend VAE75CEO25 display an additional α'_{VAE} relaxation above the glass transition that is attributed to motion in the crystalline VAE regions. The introduction of a softer component in the blend shifts the occurrence of the process to lower temperatures, and for higher CEO contents, this relaxation is not longer experimentally observed. VAE copolymers are semicrystalline at any composition [3,5], as commented in Section 1. Consequently, it is expected them to show a crystalline relaxation mechanism at temperatures higher than the relaxation associated to the glass transition, since crystallinity developed by VAE copolymers processed under usual thermal treatments is relatively high [4,21]. Nevertheless, due to the feasible interactions of their hydroxyl groups with environmental moisture if the content of water either absorbed or adsorbed is higher than a 2% in weight, this relaxation associated to motion in the crystalline regions is only intuitively observed [18] because of the plasticizing effect of the water within the amorphous phase. Our previous experience in VAE copolymers leads us to keep the blends after processing in a desiccator at room temperature and take specimens just before an experiment. Therefore, this α'_{VAE} relaxation is unambiguously seen.

3.3. Uniaxial tensile properties and microhardness

Looking first at the mechanical response under tension, Fig. 6 shows the main features found in VAE, CEO and their

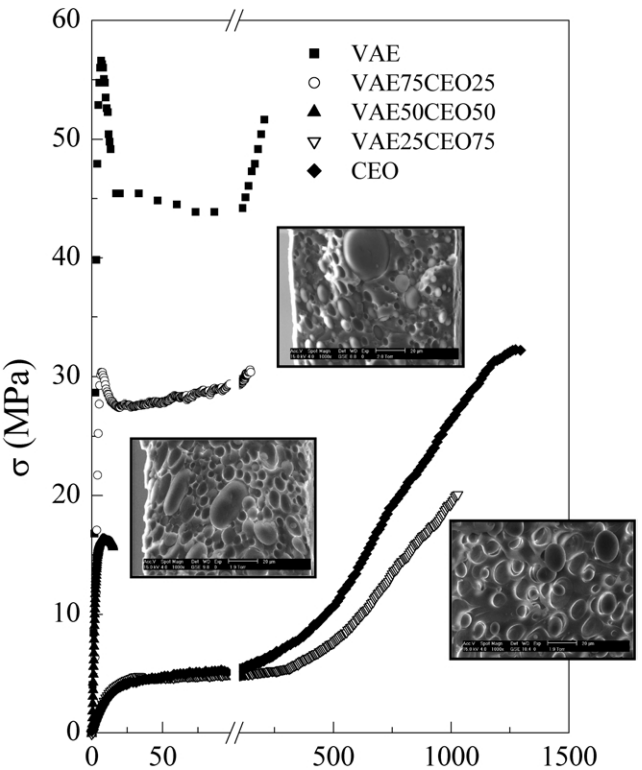

Fig. 6. Stress–strain curves for the different samples stretched at room temperature and 10 mm min^{-1} and SEM photographs (1000×, ⊢⊣ 20 μm) for the blends.

Table 4
Mechanical parameters of VAE, CEO and the different blends analyzed at 23 °C: Young's modulus, E; yield stress, σ_Y; yield deformation, ε_Y; tensile strength at break, σ_B; deformation at break, ε_B; toughness and microhardness, MH

Sample	E (MPa)	σ_Y (MPa)	ε_Y (%)	σ_B (MPa)	ε_B (%)	Toughness (kJ m^{-2})	MH (MPa)
VAE	1200	55	6.5	52	210	1425	133
VAE75CEO25	1100	29	5.5	30	150	645	87
VAE50CEO50	465	16	4	15	16	35	38
VAE25CEO75	35	4.2	10	20	1025	1500	7.7
CEO	32	4.0	15	29	1300	3250	4.9

corresponding blends. The incorporation of a plastomer in VAE decreases the stiffness of this material proportionally to the plastomer content in the blend because of the softness increase joined to the higher hindrance for establishing hydrogen bonds between hydroxyl groups. Consequently, the Young's modulus lessens as CEO content increases, as listed in Table 4. The decrease in rigidity caused by the CEO addition is also observed in the habit that deformation process takes place. VAE behaves as a typical semicrystalline polymer, i.e. the stretching process occurs by a necking formation. The yielding stress value is significantly lowered by the incorporation of a 25% in CEO which also causes the reduction of necking as determined by comparison of the yielding stress and the subsequent minimum stress value found just after its initiation. These two features are more pronounced in VAE50CEO50 since this specimen breaks before the complete establishment of the neck. On the other hand, an essentially homogeneous deformation process takes place in VAE25CEO75 because of the high elastomeric contribution stemming from CEO at room temperature. Consequently, a well-defined yield stress is not exhibited because there is not a neck formation along the deformation process, contrary to that just described in VAE, VAE75CEO25 and VAE50CEO50.

MH is other significant mechanical magnitude in polymers, which measures the resistance of the material to plastic deformation and, accordingly, provides an idea about local strain. MH involves a complex combination of properties (elastic modulus, yield strength, strain hardening, toughness). The variation of MH with the CEO content is seen in Fig. 7. As occurred for the Young's modulus and yield stress, the change is considerably dependent upon CEO content. This figure portrays that the dependence of yield stress and microhardness shows a negative deviation of the additivity rule along the composition range, whereas a positive departure of the theoretical values is found in the dependence of elastic modulus with VAE content for VAE75CEO25 (upper part of Fig. 7), probably due to role that the hydrogen bonds play in the rigidity of this blend with the largest VAE content. The VAE component acts as matrix at this composition and CEO is uniformly dispersed within it, as displayed in its corresponding SEM micrograph of Fig. 6.

Figure7 M. L. Cerrada et al.

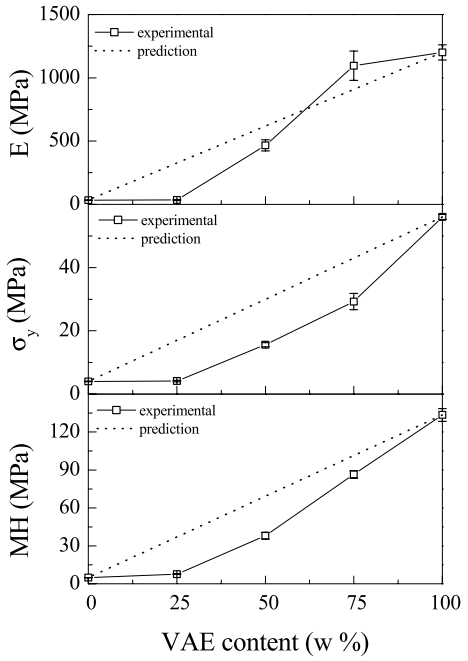

Fig. 7. Experimental and predicted (supposing a perfect mixing additivity rule) dependence of Young's modulus (upper plot), yielding stress (medium plot) and MH (lower plot) with the composition of VAE in the blends.

A direct relationship is commonly found between the Young's modulus and MH [42] and the following empirical equation has been proposed:

$$\mathrm{MH} = aE^b \tag{2}$$

where a and b are constants. This equation is also fulfilled by many systems [43–46] in a very broad range of MH and E values: from thermoplastic elastomers to very rigid polymers. Therefore, a linear relation is obtained when plotting log MH vs. log E. A good linear relationship in the log–log scale is also found in the blends under study considering either the elastic moduli obtained from uniaxial stretching or from E', as depicted in the upper plot of Fig. 8. Moreover, a straight correlation between MH and the yield stress is also exhibited in the double logarithmic representation, as seen in the lower plot of Fig. 8.

The plain CEO is a plastomer and exhibits dual characteristics of plastic and elastomeric behavior, as shown in Fig. 6. Therefore, the break elongation in CEO is very high at room temperature, reaching values close to 1300%. Due to the high elastic contribution on the overall deformation process of this copolymer, a considerable recovery is attained either after breaking or releasing specimens from the grips. In the blends, the elongation at break diminishes (Table 4) from VAE25CEO75 to VAE75CEO25, this parameter being in VAE75CEO25 even lower than in the plain VAE. At mid-content, the shortest breaking elongation is found. This feature might be explained considering the practically total incompatible nature clearly observed in the

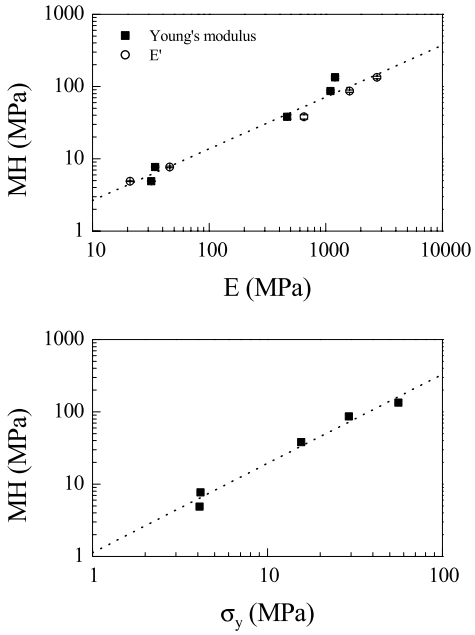

Fig. 8. Relationships between MH and either Young's modulus and E' (upper plot) or yielding stress (lower plot) in the different specimens.

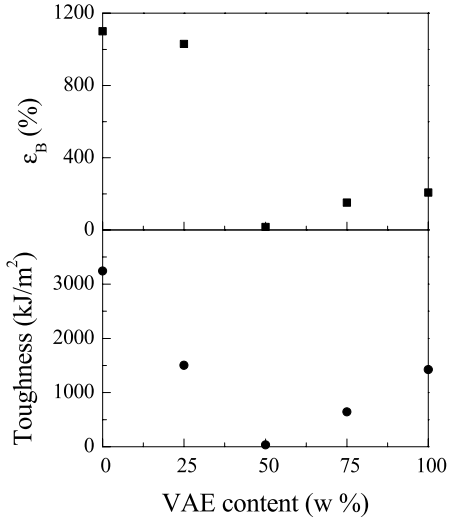

Fig. 9. Dependence of deformation at break and toughness with the VAE content.

SEM pictures obtained for these blends (Fig. 6). Two different types of droplets are observed whose size is dependent on the blend composition, and the macroscopic failure behavior is deeply affected by the morphology developed. In VAE25CEO75, CEO is the polymeric matrix and the VAE is embedded in this matrix. Therefore, the elongation at break is quite high because of CEO ductility, similarly to other relative parameters, as toughness. The concept of this mechanical parameter might be defined in several ways, one of which is in terms of the area under the stress–strain curve [47]. It is, therefore, an indication of the energy that a material can store before its rupture. The opposite situation is found in VAE75CEO25 where the minor component is CEO and, then, VAE is the continuous polymeric matrix and CEO is now the segregated component into droplets, owned to its high hydrophobicity. The introduction of a 25% in weight of CEO disrupts the whole physical network of VAE and all of the mechanical parameters are lowered compared to those found in the neat VAE. In VAE50CEO50, the existence of VAE and CEO segregation joined, probably, to the difference in the melt flow index (MFI in Table 1) of both constituents cause a matrix-particle morphology that leads to a rapid fracture because of the poor adhesion at the interface between the two components. Consequently, elongation at break and toughness show the lower values at this content (Fig. 9).

In summary, each constituent in VAE/CEO blends crystallizes in its particular crystalline cell and an almost weighed superposition of their WAXS profiles is observed. The similarity of both lattices provokes that diffraction peaks arising from VAE and CEO appear at the same spacings region. Same analogy is also found from the analysis of SAXS profiles and, then, these two types of crystallites developed in the blends show rather close long spacing values. However, DSC results indicate an inhibition in VAE crystallization by introduction of CEO, that is very slight in VAE75CEO25 and VAE50CEO50 and considerably more important in VAE25CEO75. Therefore, location of the melting temperature, T_m, concerning VAE component is shifted to lower temperatures, and the melting enthalpy normalized respect to the VAE content is diminished as CEO increases in the blend. On the other hand, a great complexity is observed in the viscoelastic response of these blends because of their multi-phasic nature and the motions that take place in each of these phases. Consequently, five different relaxation processes are observed, two of them being related to cooperative motions in the amorphous regions of each of the components. The practically constancy in the location of these two mechanisms related to the T_gs confirm the incompatibility of the two components. The different mechanical behavior presented by the two neat copolymers leads to deep changes as CEO content increases in the blend. The introduction of this hydrophobic constituent hinders the establishment of intra and intermolecular hydrogen bonds, provoking a diminution of the stiffness and, consequently, of all of the mechanical parameters associated to this magnitude as elastic modulus, yield stress and microhardness. This disruption of the physical network within VAE copolymer gives also rise to a deep change in oxygen permeability, as seen in Fig. 10 and discussed widely in a previous article [17]. A variation of nearly three decades is found passing from neat VAE to VAE75CEO25. The poor adhesion at the interface between the two components requires a further investigation in order to be able to design tailor-made oxygen barrier materials with good mechanical performance. The development of compatibilizing agents is demanded for obtaining positive deviation of the simple additivity rule and enhancing continuity at interfaces. It seems that those agents able to

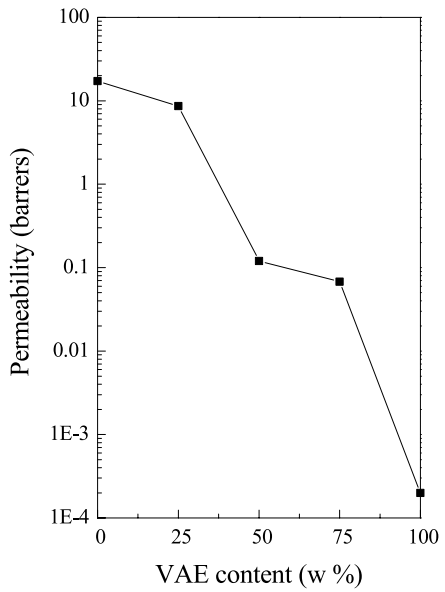

Fig. 10. Dependence of oxygen permeability, at 30 °C, with the VAE content. The value for neat VAE copolymer has been taken from the literature [5].

form hydrogen interactions would constitute the best option at first approximation. Finally, CEO might improve some of the processing deficiencies exhibited by VAE copolymers, due to its plastomer character.

Acknowledgements

The financial support of Comunidad Autónoma de Madrid and Ministerio de Ciencia y Tecnología (Projects 07G/0038/2000 and MAT2001-2321, respectively) is gratefully acknowledged. The synchrotron work (in the polymer line A2 of HASYLAB at DESY, Hamburg) was supported by the IHP Programme 'Access to Research Infrastructures' of the European Commission (Contract HPRI-CT-1999-00040/2001-00140). The authors thank the collaboration of the Hasylab personnel, specially Dr A. Meyer and Dr S. Funari.

References

[1] Bunn CW, Peiser HS. Nature 1947;159:161.
[2] VanderHart DL, Simmons S, Gilman JW. Polymer 1995;36:4223.
[3] Nakamae K, Kameyama M, Matsumoto T. Polym Engng Sci 1979;19:572.
[4] Cerrada ML, Pérez E, Pereña JM, Benavente R. Macromolecules 1998;31:2559.
[5] Dunn AS. In: Finch CA, editor. Polyvinyl alcohol-developments. London: Wiley; 1992. p. 217–38.
[6] Blackwell AL, Plastic film technology, high barrier plastic films for packaging, vol. 1. Lancaster, PA: Technomic; 1989. p. 41.
[7] Chou R, Lee IHJ. Plast Films Sheeting 1997;13:74.
[8] Faisant JB, Aït-Kadi A, Bousmina M, Deschênes L. Polymer 1998;39:533.
[9] Yeo JH, Lee ChH, Park Ch-S, Lee K-J, Nam J-D, Kim SW. Adv Polym Technol 2001;20:191–201.
[10] Gopalakrishnam R, Schultz JM, Bohil R. J Appl Polym Sci 1995;56:1749.
[11] Kit KM, Schultz JM, Golhil R. Polym Engng Sci 1995;35:680.
[12] Akiba I, Akiyama S. Polym J 1994;26:873.
[13] Lagaron JM, Jiménez E, Saura JJ, Gavara R. Polymer 2001;42:7381.
[14] Speed CS, Trudell BC, Mehta AK, Steininger FJ. RETEC polyolefins VII, Society of Plastics Engineers; 1991, p. 45.
[15] Laguna MF, Cerrada ML, Benavente R, Pérez E. J Membr Sci 2003;212:167–76.
[16] Laguna MF, Cerrada ML, Benavente R, Pérez E. J Polym Sci, Polym Phys 2003;41:2174–84.
[17] Laguna MF, Cerrada ML, Benavente R, Pérez E. J. Polym. Sci. Polym. Phys. Submitted for publication.
[18] Cerrada ML, Pereña JM, Benavente R, Pérez E. Polymer 2000;41:6655–61.
[19] Cerrada ML, Pereña JM, Benavente R, Pérez E. Polym Engng Sci 2000;40:1036–45.
[20] Cerrada ML, Benavente R, Pérez E. J Mater Res 2001;16:1103.
[21] Cerrada ML, Benavente R, Pérez E, Pereña JM. J Polym Sci, Polym Phys 2001;39:1–12.
[22] Prieto O, Pereña JM, Benavente R, Cerrada ML, Pérez E. Macromol Chem Phys 2002;203:1844.
[23] Cerrada ML, Benavente R, Pérez E, Moniz-Santos J, Ribeiro MR. Polymer 2001;42:7197.
[24] Vanden Eynde S, Mathot VBF, Koch MHJ, Reynaers H. Polymer 2000;41:4889.
[25] Cerrada ML, Benavente R, Pérez E. Macromol Chem Phys 2002;203:718–26.
[26] Cerrada ML, Benavente R, Peña B, Pérez E. Polymer 2000;41:5957–65.
[27] Schatzki TF. J Polym Sci 1962;57:496.
[28] Arridge RGC. Rev Deform Behav Mater 1981;3:249.
[29] Boyd RH. Polymer 1985;26:1123.
[30] Boyer RF. Rubber Chem Technol 1963;36:1303.
[31] Boyd RH, Breitling RS. Macromolecules 1974;7:855.
[32] Boyd RH. J Polym Sci, Polym Phys 1975;13:2345.
[33] Heaton NJ, Benavente R, Pérez E, Bello A, Pereña JM. Polymer 1996;37:3791.
[34] Boyd RH, Gee RH, Han J, Jin Y. J Chem Phys 1994;101:788.
[35] Jin Y, Boyd RH. J Chem Phys 1998;108:9912.
[36] Yamaguchi M, Miyata H, Nitta K. J Appl Polym Sci 1996;62:87.
[37] Boyd RH. Macromolecules 1984;17:903.
[38] Han J, Gee RH, Boyd RH. Macromolecules 1994;27:7781.
[39] Popli R, Mandelkern L. Polym Bull 1983;9:260.
[40] Popli R, Glotin M, Mandelkern L, Benson RS. J Polym Sci, Polym Phys 1984;22:407.
[41] Rotter G, Ishida H. Macromolecules 1992;25:2170–6.
[42] Baltá-Calleja FJ. Adv Polym Sci 1985;66:117.
[43] Lorenzo V, Pereña JM, Fatou JMG. Makromol Chem 1989;172:25.
[44] Benavente R, Pérez E, Quijada R. J Polym Sci, Polym Phys 2001;39:277.
[45] Cerrada ML, de la Fuente JL, Fernández-García M, Madruga EL. Polymer 2001;42:4647.
[46] Cerrada ML, de la Fuente JL, Madruga EL, Fernández-García M. Polymer 2002;43:2803–10.
[47] Duckett RA. In: Ward IM, editor. Structure and properties of oriented polymers. London: Applied Science Publishers; 1975. Chapter 11.